The EMBO Journal vol.15 no.11 pp.2678–2684, 1996

Crystal structure of human lithostathine, the pancreatic inhibitor of stone formation

Jay A.Bertrand, David Pignol, Jean-Paul Bernard[1], Jean-Michel Verdier[1], Jean-Charles Dagorn[1] and Juan Carlos Fontecilla-Camps[2]

Laboratoire de Cristallographie et Cristallogénèse des Protéines, Institut de Biologie Structurale J.P. Ebel, CEA-CNRS, 41 avenue des Martyrs, 38027 Grenoble Cedex 1 and [1]Institut National de la Santé et de la Recherche Médicale, U. 315-F-13009 Marseille, France

[2]Corresponding author

J.A.Bertrand and D.Pignol contributed equally to this work

Human lithostathine (HLIT) is a pancreatic glycoprotein which inhibits the growth and nucleation of calcium carbonate crystals. The crystal structure of the monomeric 17 kDa HLIT, determined to a resolution of 1.55 Å, was refined to a crystallographic R-factor of 18.6%. Structural comparison with the carbohydrate-recognition domains of rat mannose-binding protein and E-selectin indicates that the C-terminal domain of HLIT shares a common architecture with the C-type lectins. Nevertheless, HLIT does not bind carbohydrate nor does it contain the characteristic calcium-binding sites of the C-type lectins. In consequence, HLIT represents the first structurally characterized member of this superfamily which is not a lectin. Analysis of the charge distribution and calculation of its dipole moment reveal that HLIT is a strongly polarized molecule. Eight acidic residues which are separated by regular 6 Å spacings form a unique and continuous patch on the molecular surface. This arrangement coincides with the distribution of calcium ions on certain planes of the calcium carbonate crystal; the dipole moment of HLIT may play a role in orienting the protein on the crystal surface prior to the more specific interactions of the acidic residues.

Keywords: antifreeze protein/calcite/chronic calcifying pancreatitus/c-type pectin/reg protein

Introduction

Pancreatic juice is characterized by high concentrations of calcium and carbonate ions at a level in which calcium carbonate crystals can spontaneously form (Moore and Vérine, 1987). However, calcium carbonate crystals are only observed in significant numbers in the juice of patients with chronic calcifying pancreatitis (CCP), a lithogenic disorder characterized by the presence of stones obstructing the pancreatic ducts, and remain scarce in juice collected from healthy individuals (De Caro *et al.*, 1988). Several lines of evidence indicate that the inhibition of calcium carbonate crystal nucleation and growth in human pancreatic juice is exerted by a 17 kDa glycoprotein named lithostathine (HLIT). For example, patients suffering from CCP have an abnormally low concentration of HLIT (Bernard *et al.*, 1995). In addition, immunofluorescence experiments have shown that HLIT binds to the surface of calcium carbonate crystals, providing an explanation for the inhibitory effects (Bernard *et al.*, 1992).

The first 11 N-terminal residues of HLIT can be removed by tryptic cleavage, producing a peptide that shows a residual activity on the inhibition and growth of calcium carbonate crystals (Bernard *et al.*, 1992). However, optimal activity can only be obtained with the entire protein, which shows an activity 100-fold greater than that of the 11-residue peptide (S.Geider, A.Baronnet, S.Nitsche, J.-P.Astier, R.Michel, R.Boistelle, Y.Berland, J.-C.Dagorn and J.-M.Verdier, in preparation). Consequently, it is likely that both the N-terminal peptide and the C-terminal domain bind to calcium carbonate crystals; a conclusion reinforced by the fact that C-terminal proteolytic fragment (residues 12–144) is a major component of pancreatic stones (De Caro *et al.*, 1988).

A multifunctional character of HLIT is suggested by the fact that from amino acid sequence comparisons, it is known now that HLIT is identical to two other functionally different proteins (Stewart, 1989), *reg* protein (Terazono *et al.*, 1988) and pancreatic thread protein (PTP; Gross *et al.*, 1985). Pancreatic islets regeneration can be induced in 90% depancreatized rats by administration of poly(ADP-ribose) inhibitors such as nicotinamide. During the process of screening the regenerating islet cDNA a novel gene, named *reg* (i.e. regenerating gene), was identified that was expressed in the regenerating islets but not in the normal islets (Terazono *et al.*, 1988). Immunohistochemical analysis of rat pancreas indicated the presence of *reg* protein in normal acinar cells and in the regenerating state in islet as well as in acinar cells. The human homologue to rat *reg* cDNA was isolated from a pancreas-derived cDNA library (Itoh *et al.*, 1990). In humans, *reg* mRNA is present in tumorial tissue of the colon and the rectum although it was not observed in the corresponding mucosae (Watanabe *et al.*, 1990).

PTP, a protein identical to the cleaved form of HLIT, was recognized in pancreatic extracts as a result of the proteins ability to undergo a freely reversible, pH dependent, fibril-globular transformation. Between pH 5.4 and 9.2, human PTP is stable in the form of uniform 7–10 nm long single threads (Gross *et al.*, 1985). Subsequent immunogenic analysis recognized a neuronal form of thread protein present in the brains of Alzheimer's disease patients that shares several antigenic epitopes with PTP (Ozturk *et al.*, 1989; De la Monte *et al.*, 1990).

The C-terminal part of HLIT is homologous with the animal C-type lectins (Patthy, 1988), showing the highest percentage of homology with the rat cartilage proteoglycan and the human IgE receptor (Petersen, 1988). Amino acid

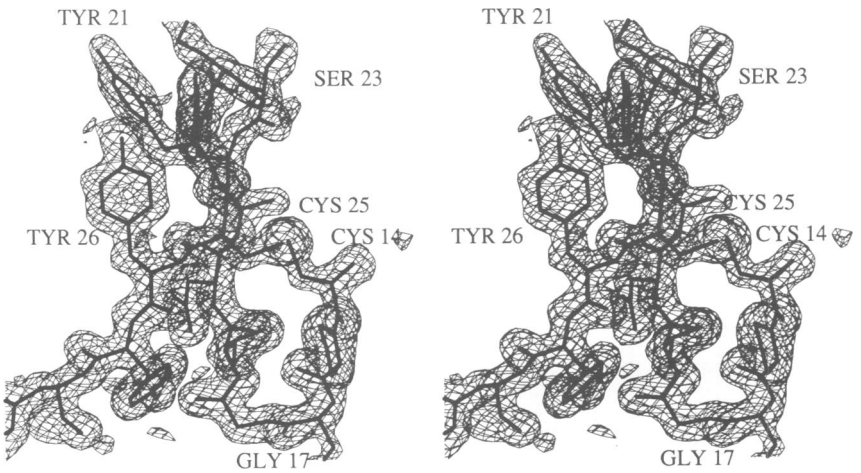

Fig. 1. View of the final ($2F_o$–F_c) electron density map contoured at 1σ around Cys14, the first N-terminal residue of the HLIT model.

similarities are distributed over regions corresponding to the consensus carbohydrate-recognition domain (CRD) and two of the three disulfide bridges in HLIT are conserved in the C-type lectin sequence motif (Drickamer, 1993). The C-type lectins are one characteristic class of the family of animal lectins, non-enzymatic calcium-dependent proteins which selectively bind to specific carbohydrate structures (Drickamer, 1988). Although HLIT shares sequence homology with the CRD of C-type lectins, no carbohydrate ligands of HLIT have been identified even though attempts have been made with numerous carbohydrate molecules (Iovanna *et al.*, 1993).

The inhibition of crystal nucleation and growth is a property of HLIT that is shared by the antifreeze proteins (AFPs). The AFPs are synthesized and secreted in the liver of marine fishes to provide protection from freezing environments and are classified into three groups (Davies and Hew, 1990); type I (helical peptides, M_r 3–5 K), type II (cysteine-rich, M_r 14 K), and type III (predominantly β-sheet, M_r 6–7 K). The type II AFPs are homologous to HLIT, showing sequence similarities distributed over both the N- and C-terminal domains. In addition, all of the cysteines responsible for disulfide bridge formation in HLIT are conserved in the reported sequences of type II AFPs (Ewart *et al.*, 1992; Ng and Hew, 1992).

We have recently obtained crystals of an *O*-glycosylated isoform of HLIT (Pignol *et al.*, 1995). Here we report the three-dimensional structure of this form of HLIT at 1.55 Å resolution, as solved by the single isomorphous replacement plus anomalous dispersion (SIRAS) method. Three-dimensional structure comparisons reveal that HLIT belongs to a large structural family which includes C-type lectins. In addition, based on the structure of HLIT, we propose a putative mechanism of interaction between HLIT and calcium carbonate.

Results and discussion

Quality of the model

The final model, which includes residues 14–144 and 137 solvent molecules, has a crystallographic *R*-factor of 18.6% (R_{free} = 24.4%; Brünger, 1992a) for all 19 532 reflections in the resolution range of 8.0–1.55 Å. The root mean square (r.m.s.) deviations are 0.01 Å from ideal bond lengths and 2.1° from ideal bond angles. The Ramachandran plot (Ramachandran *et al.*, 1963) for the final model shows 88.6% of the residues in the most favoured regions and none of the non-glycine residues in the disallowed regions.

The first 13 residues, including the *O*-glycosylation site, Thr5, are disordered in the crystal. Although the first N-terminal residue of our model (Cys14) is well defined in electron density (Figure 1), no electron density is present for the adjacent N-terminal residues. Crystal packing analysis indicates that these residues could protrude into a large solvent channel present in the crystal. Proteolytic cleavage after the susceptible Arg11 can be ruled out as an explanation for the missing residues since mass spectroscopic analysis of the crystallized protein indicates the presence of the complete 17 kDa polypeptide. In an effort to locate the first 13 N-terminal amino acid residues, the final model was refined against X-ray data collected at 113 K. Although at this temperature thermal disorder should be minimal, no density corresponding to the missing amino acids was observed. This indicates that residues 1–13 are statically disordered in the crystal.

Overall protein structure

HLIT has the shape of a heart with dimensions 45×30×25 Å (Figure 2). The protein folds into one globular domain that consists of three helices and six β-strands, the latter forming two antiparallel β-sheets. The sequential connectivity follows the scheme β1–β2–α1–α2–β3–β4–α3–β5–β6 (Figure 3). The first well-defined N-terminal residue of the structure participates in an intramolecular disulfide bond (Cys14–Cys25; Figure 1) forming a loop. This loop contains a short β-strand (β1; residues 19–21) which forms an anti-parallel β-sheet with strands β2 and β6. The two major helices α1 and α2, of respectively three and four helical turns, are oriented perpendicular to one another framing the three β-strands (β1, β2 and β6) of the lower half of the molecule (Figure 2). The Cys42–Cys140 disulfide bridge connects α1 to β6. The upper half of the molecule includes the other three β-strands (β3, β4 and β5). Two strands of this second antiparallel β-sheet, β4 and β5, are separated by a single helical turn

(α3) and are connected at one extremity by the Cys115–Cys132 disulfide bridge. In addition to the secondary structure elements, the structure also contains several extended loops and stretches of non-regular secondary structure which represent >60% of the molecule.

Structural comparisons

The overall folding of HLIT, from residues 26 to 144, is similar to the C-type lectin domains of rat mannose-binding protein (RMBP) and human E-selectin (HESL)

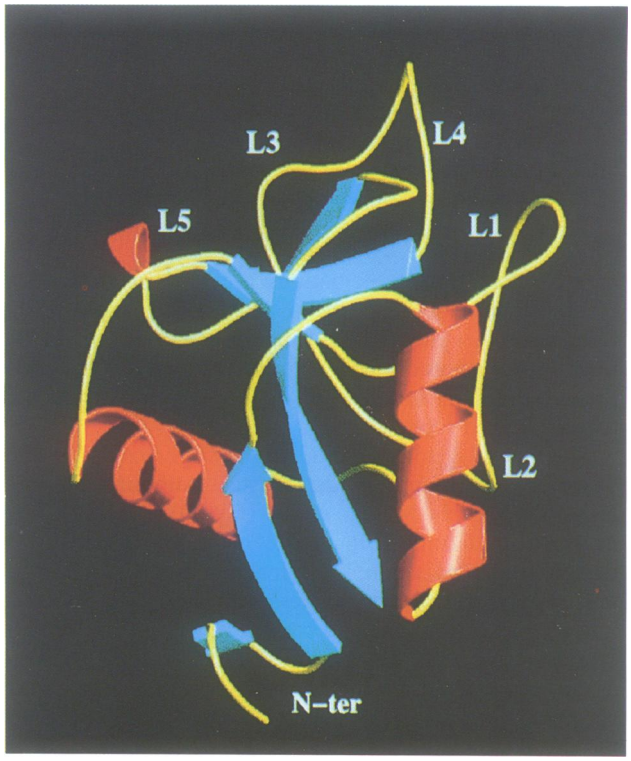

Fig. 2. Ribbon diagram of HLIT produced with the program Molscript (Kraulis, 1991).

(Weis *et al.*, 1991, 1992; Graves *et al.*, 1994). Although the sequence identity between HLIT and RMBP or HESL is only 19% (Table I), superposition of the three structures indicates a common architecture (Figure 4). The r.m.s. differences in α carbon positions between the 109 matched residues of HLIT and RMBP, or HESL are 1.5 and 1.6 Å, respectively. These relatively high values reflect the structural variations in the regions of loops and turns. Comparison of HLIT with RMBP and HESL reveals an additional turn in the second α-helix (residues 56–68) and differences in the conformation of three of the five loops (Figure 4). Loop one of HLIT contains Pro83 which results in the loop folding back towards the centre of the molecule. Loop four of HLIT is in a twisted conformation with respect to the corresponding loops in RMBP and HSEL. In HLIT, the conformational difference of loop four with respect to RMBP and HESL can be explained

Table I. Amino-acid sequence alignment of HLIT with related proteins

hlit	1	QEAQTELPQARISCPEGTNAYRSYCYYFNEDREE	33
rmbp	109	----------KKFFVTNHERM	119
hesl	1	----------WSYNTSTEAMT	11
rave	1	-------NRAPPNCPAGWQPLGDRCIYYETTAM	26
hlit	34	TWVDADLYCQNMNSGNLVSVLTQAEGAFVASLI	66
rmbp	120	PFSKVKALCSEL-RGTVAIPRNAEENKAIQEVA	151
hesl	12	YDEAS-AYCQQRYTH-LVAIQNKEEIEYLNSIL	42
rave	27	TWALAETNCMKLGGH-LASIHSQEEHSFIQTLN	58
hlit	67	KESGTDDFNVWIGLHDPKKNRRWHWSSGSL-VS	98
rmbp	152	K-----T-SAFLGITDEVTEGQFMYVTG-GRLT	177
hesl	43	SYS--PS-YYWIGIRKVNNVWVWVGTQKPLTEE	72
rave	59	AGV------VWIGGSACLQAGAWTWSDGTP-MN	84
hlit	99	YKSWGIGAPSSVN-PGYCVSLTSSTGFQK--WK	128
rmbp	178	YSNWKKDEPNDHGSGEDCVTIVD--N-GL--WN	205
hesl	73	AKNWAPGEPNNRQKDEDCVEIYIKREKDVGMWN	105
rave	85	FRSWCSTKPDDVLA-ACCMQMTAA-ADQC--WD	113
hlit	129	DVPCEDKFSFVCKFKN	144
rmbp	206	DISCQASHTAVCEFPA	221
hesl	106	DERCSKKKLALCYTAA	121
rave	114	DLPCPASHKSVCAMTF	129

C-type lectin RMBP and HESL sequences were aligned to that of HLIT using three-dimensional structural similarities. Sea raven AFP protein amino acid sequence (rave) was manually aligned to that of HLIT.

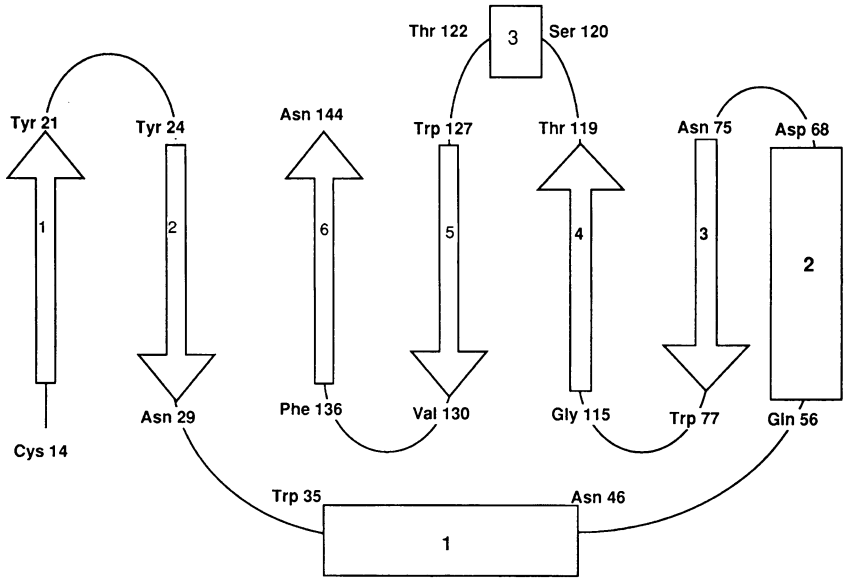

Fig. 3. Schematic diagram of HLIT polypeptide topology. The β-strands are depicted as arrows, with the arrowheads indicating the direction of the chain. α-Helices are shown as rectangles.

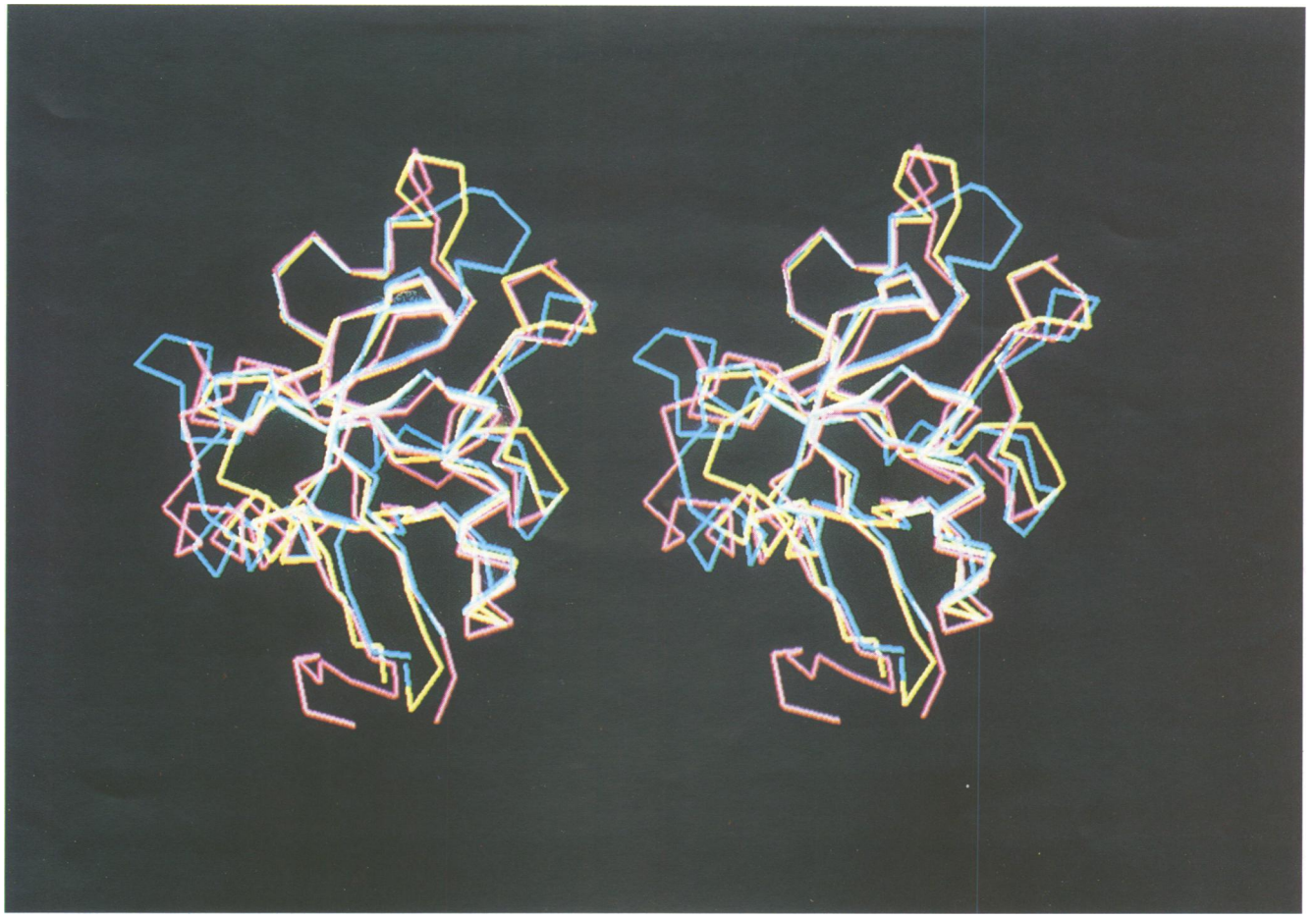

Fig. 4. A stereo view of the optimal α-carbon superposition of the C-type lectin domains of RMBP (Weis *et al.*, 1992) and HESL (Graves *et al.*, 1994) onto HLIT. RMBP is coloured in blue, HESL in yellow and HLIT in pink.

by the presence of Pro112 and the fact that the loop is one residue shorter.

As a consequence of both sequence (Table I) and structural differences, the two calcium-binding sites present in mannose-binding protein (Figure 5), and the one in HESL are not present in HLIT (Weis *et al.*, 1991, 1992; Graves *et al.*, 1994). Site one, which is formed by residues contained in loops one and four, has only been observed in the mannose-binding proteins. This potential site in HLIT is lost due to: (i) differences in the position of loop one which result in the side-chain of Asn86 pointing away from the potential site and the side chain of the adjacent residue, Arg87, being inserted into the site. Atom NH1 of Arg87 replaces the calcium ion in some respects by hydrogen-bonding to the carbonyl oxygen of Gly113 and to Oγ of one of the two side-chain conformations of Asp82. (ii) Differences in the position of loop four which result in no residue being topologically equivalent to Asp188 of RMBP. (iii) Sequence differences in HLIT which do not provide calcium ligands; Asp194 of RMBP corresponds to Tyr114 in HLIT. In RMBP, the second calcium-binding site is formed by residues contained in β5 and loops three and four. In contrast to what is observed for site one, the α-carbons for the residues which form site two in RMBP and HESL are topologically equivalent to the corresponding residues of HLIT. This implies that site two is lost as a result of differences in the amino acid sequence. RMBP residues Glu185, Asn187, Glu193, Asn205 and Asp206 correspond, respectively, to HLIT residues Ala106, Ser108, Gly113, Lys128 and Asp129. Structural evidence for the loss of site two in HLIT is consistent with the absence of carbohydrate-binding activity (Iovanna *et al.*, 1993).

A large structural family with a variety of functions

HLIT and the C-type lectins differ at two levels: the extreme conformational flexibility of the N-terminal segment of HLIT (residues 1–13) and the lack of both calcium- and carbohydrate-binding sites. C-type lectins are in general modular with one domain assuring the carbohydrate-binding properties and another one serving a structural role. In RMBP, a trimeric protein, each polypeptide chain contains a collagen-like region (17 Gly–Xaa–Yaa triplets), linked by a short helical stretch of 34 amino-acids (the 'neck' region) to a C-terminal, C-type lectin domain (Sheriff *et al.*, 1994; Weis and Drickamer, 1994). It is this 'neck' region of RMBP that facilitates the characteristic trimer formation. In the monomeric HLIT, the ability to interact with calcium carbonate crystals is due to both the C- (CRD domain from residues 26 to 144) and N-terminal (from residue 1 to 25) part of the molecule. As a result, it can be concluded that the topology initially described for the C-type lectins defines a much

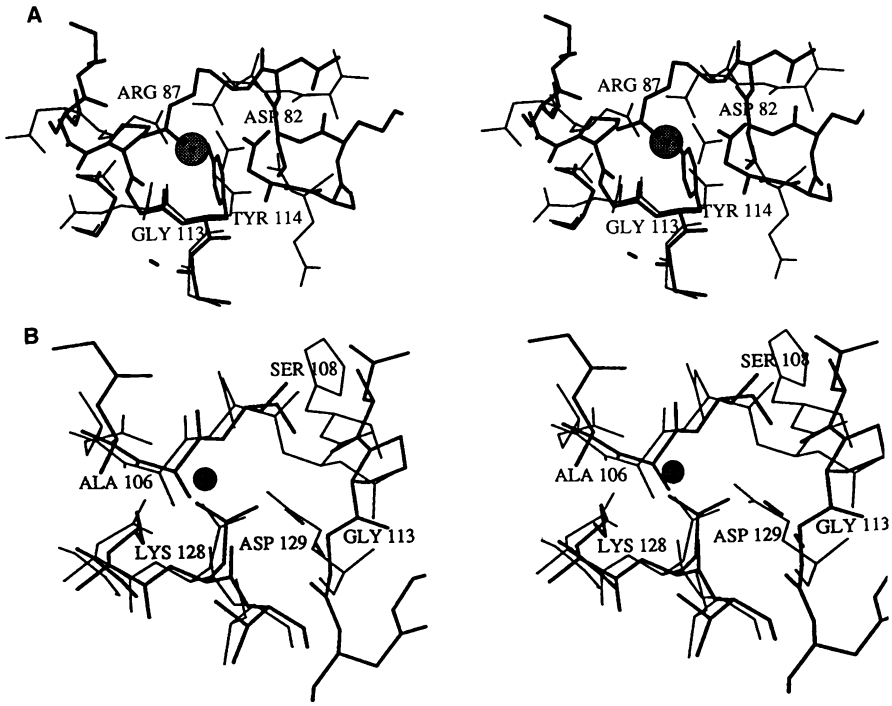

Fig. 5. Stereo diagrams showing the superposition of the calcium-binding sites of RMBP (Weis *et al.*, 1992) onto HLIT. RMBP is shown by thin lines. The calcium present in the RMBP structure is represented by a sphere. (**A**) Calcium-binding site one. (**B**) Calcium-binding site two.

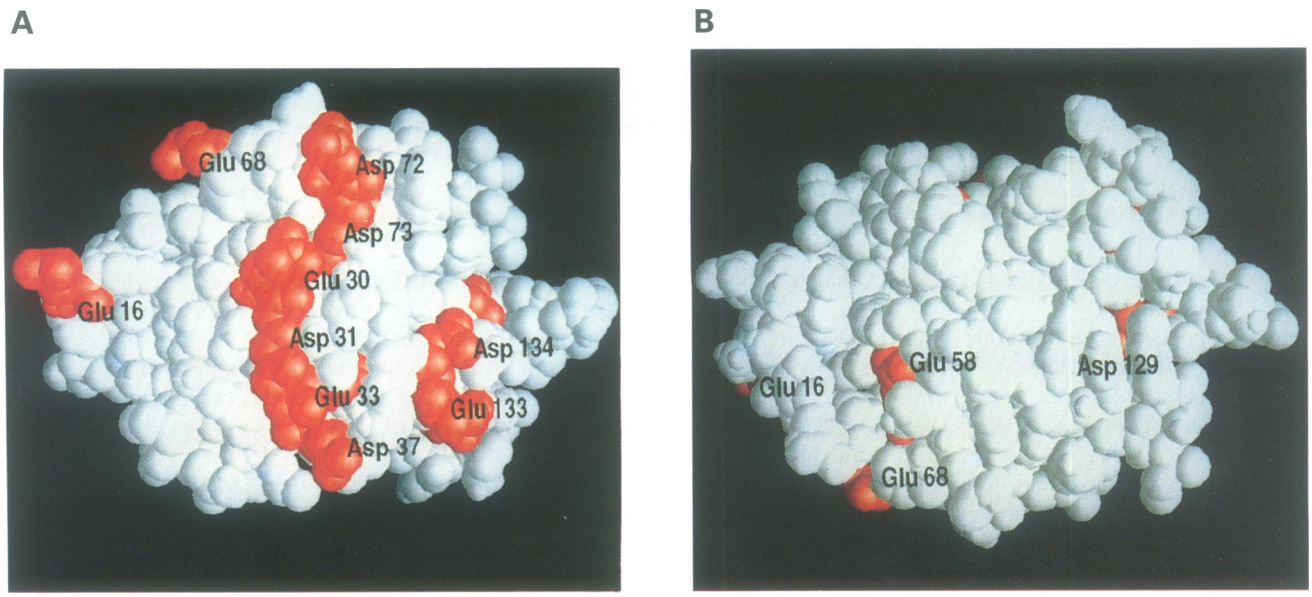

Fig. 6. Ball and stick representation of two opposite sides of HLIT, obtained by 180° rotation about the *x*-axis. Acidic residues are shown in red and all other residues in white. Pictures were drawn using the program GRASP (Nicholls *et al.*, 1991).

larger structural family with a variety of functions which includes the C-type lectins and HLIT.

A highly polarized molecule

HLIT reveals a unique distribution of charged residues on the surface (Figure 6). On one side of the molecule (Figure 6A), the surface of the protein presents two solvent-exposed acidic stretches including nine of the 14 acidic residues (Glu30, Asp31, Glu33, Asp37, Asp72, Asp73, Glu133, Asp134 and Asp129); the opposite side contains only two acidic residues (Glu58 and Glu68; Figure 6B). On the more acidic side, aspartic and glutamic residues are clustered in two contiguous parallel stretches of 22 and 12 Å long. The stretches, which are separated by ~10 Å, traverse the surface of the protein. The longest acidic network is made of six residues, four of them belonging to the β2–α1 loop (Glu30, Asp 31, Glu33 and Asp37) and the remaining two belonging to α2–β3 loop (Asp72 and Asp73). The continuity of the stretch is maintained by the roughly constant 6 Å distance which separates each acidic residue (the five interconnecting Cβ–Cβ distances are between 5.83 and 6.08 Å). The second acidic stretch is made of three residues from the β5–β6 loop (Asp129, Glu133 and Asp134). In addition to this

unique structural organization of acidic residues, HLIT presents a heterogenous distribution of basic residues. Out of the 13 lysine or argine residues, only three (Arg32, Lys135 and Lys128) are exposed on the acidic surface. Although the relative position of the basic residues seems to lack organization, the overall distribution of charged residues leads to a highly polarized structure. The dipole moment, calculated with the program GRASP (Nicholls *et al.*, 1991), is perpendicular to the plane formed by the acidic residues and is five times greater than that of RMBP and HESL.

Towards a general protein–crystal interaction mechanism

The acidic stretches could be responsible for the binding of HLIT to calcite. The implication of acidic residues in protein-calcium carbonate crystal interactions has been previously suggested for the acidic glycoproteins involved in exoskeleton development (Berman *et al.*, 1988). The ~6 Å distance interval between the residues of the acidic cluster reflects a periodicity compatible with the distribution of calcium ions on several planes of the calcite crystal. The dipole moment of HLIT may play a role in orienting the protein on the crystal surface prior to the more specific interactions of the acidic residues.

HLIT shows 29% sequence identity with sea raven AFP (Ng and Hew, 1992), a type II AFP (Davies and Hew, 1990). This value is greater than the ones obtained when comparing HLIT with either RMBP or HESL (19% in both cases). The amino acid sequence alignment of HLIT and sea raven AFP shows that many of the conserved residues are either cysteines, glycines or bulky aromatic residues (Table I). Furthermore, the N-terminal disulfide loop of HLIT, which is not conserved in RMBP and HESL, is also present in sea raven AFP (Ng and Hew, 1992).

The mechanisms responsible for HLIT-calcium carbonate interactions and AFP–ice interactions may be similar in some respects. In general, the AFP–ice interactions are believed to occur through a combination of hydrogen bonds and dipole interactions. In the type I AFPs, the ice-binding surface is suggested by a linear, repetitive, hydrogen-bonding motif (Yang *et al.*, 1988; Sicheri and Yang, 1995). Hydrogen-bonding residues from the C-terminal β-sheet of a type III AFP have also been postulated to be responsible for the antifreeze activity (Sönnichsen *et al.*, 1993; Chao *et al.*, 1994). These hydrogen-bonding motifs may play a similar role to the one assigned here to the acidic clusters present in HLIT.

Little is currently known about the specific interactions between ice and the type II AFPs. Amino acid sequence similarities with HLIT suggest a common folding for the two molecules. This has been confirmed by a model of sea raven AFP, constructed from the coordinates of RMBP using comparative modelling methods (Sönnichsen *et al.*, 1995). Topologically equivalent ice and calcite-binding sites in the two proteins would require the presence of a patch of hydrogen-bond forming residues in the former. A protein–ice interaction site has been proposed from the model of sea raven AFP and is roughly located on the same side of the molecule as the corresponding acidic patch of HLIT. However, the location of an exact protein–ice interaction site can only be verified by amino acid mutations because of the large number of hydrophillic residues present on the surface of protein molecules.

The crystal structure of HLIT shows that what has been described as typical of the C-type lectin structure is a much more general topology which includes the lectins, the type II AFPs and HLIT. As more proteins belonging to this structural family are investigated a clearer picture of their origin should emerge.

Materials and methods

HLIT was purified and crystallized as described previously (Pignol *et al.*, 1995). Crystals belong to the hexagonal space group $P6_5$ with unit cell dimensions $a = b = 47.19$ Å and $c = 108.66$ Å. A complete native data set has been collected to 1.5 Å (Pignol *et al.*, 1995). A detailed description of the structure determination procedure will be reported elsewhere. All data sets were collected on a MarResearch imaging plate system mounted on the wiggler line W32 at the LURE synchrotron radiation facility (Orsay, France). Data were integrated using the program MOSFLM (Leslie, 1987), and then reduced using CCP4 programs ROTAVATA and AGROVATA (CCP4, 1994). After screening many heavy atom derivatives, only one (para-chloromercuribenzene sulfonic acid) proved to be useful. Data from this derivative were collected to 1.7 Å resolution and used to calculate SIRAS phases to 2.5 Å resolution, that were improved by solvent flattening and histogram matching with the program SQUASH (Zhang, 1993). The high quality of the improved electron density in conjunction with the amino-acid sequence (De Caro *et al.*, 1987) allowed an unambiguous tracing of the main chain with the program O (Jones *et al.*, 1991). Structure refinement was performed with X-PLOR (Brünger, 1992b), applying the parameter set of Engh and Huber (1991). The final coordinates have been deposited with the Brookhaven Protein Data Bank and will be released six months after publication.

Acknowledgements

The assitance of Drs J.P.Benoit and R.Fourme of the W32 station of the LURE synchrotron radiation facility is gratefully acknowledged. Dr Eric Forest (LSM/IBS) is thanked for performing the mass spectrometry experiment. J.A.B was the recipient of a 'Collaborateur temporaire étranger' fellowship from the Commissariat à l'Energie Atomique, France. This work was supported by the Commissariat à l'Energie Atomique and the Centre National de la Recherche Scientifique.

References

Berman,A., Addadi,L. and Weiner,S. (1988) Interactions of sea-urchin skeleton macromolecules with growing calcite crystals—a study of intracrystalline proteins. *Nature*, **331**, 546–548.

Bernard,J.P., Adrich,Z., Montalto,G., De Caro,A., De Reggi,M., Sarles,H. and Dagorn,J.C. (1992) Inhibition of nucleation and crystal growth of calcium carbonate by human lithostathine. *Gastroenterology*, **103**, 1277–1284.

Bernard,J.-P., Barthet,M., Gharib,B., Michel,R., Lilova,A., Sabel,J., Dagorn,J.-C. and De Reggi,M. (1995) Quantification of human lithostathine by high performance liquid chromotography. *Gut*, **36**, 630–636.

Brünger,A.T. (1992a) Free *R* value: a novel statistical quantity for assesing the accuracy of crystal structures. *Nature*, **355**, 472–475.

Brünger,A.T. (1992b) X-PLOR Version 3.1: A System for X-ray Crystallography and NMR. Yale University Press, New Haven, CT.

Chao,H., Sönnichsen,F.D., DeLuca,C.I., Sykes,B.D. and Davies,P.L. (1994) Structure-function relationships in the globular type III antifreeze protein: Identification of a cluster of surface residues required for binding to ice. *Protein Sci.*, **3**, 1760–1769.

Collaborative Computational Project. No. 4 (1994) The CCP4 suite: programs for protein crystallography. *Acta Crystallogr.*, **D50**, 760–763.

Davies,P.L. and Hew,C.L. (1990) Biochemistry of fish antifreeze proteins. *FASEB J.*, **4**, 2460–2468.

De Caro,A., Multignier,L., Dagorn,J.C. and Sarles,H. (1988) The human pancreatic stone protein. *Biochimie*, **70**, 1209.

De Caro,A.M., Bonicel,J.J., Rouimi,P., De Caro,J.D., Sarles,H. and Rovery,M. (1987) Complete amino acid sequence of an immuno-

reactive form of human pancreatic stone protein isolated from pancreatic juice. *Eur. J. Biochem.*, **168**, 201–207.
De la Monte,S.M., Ozturk,M. and Wands,J.R. (1990) Enhanced expression of an exocrine pancreatic protein in Alzheimer's disease and the developing human brain. *J. Clin. Invest.*, **86**, 1004–1013.
Drickamer,K. (1988) Two distinct classes of carbohydrate-recognition domains in animal lectins. *J. Biol. Chem.*, **263**, 9557–9560.
Drickamer,K. (1993) Ca^{2+}-dependent carbohydrate-recognition domains in animal proteins. *Curr. Opin. Struct. Biol.*, **3**, 393–400.
Engh,R.A. and Huber,R. (1991) Accurate bond and angle parameters for X-ray protein structure refinement. *Acta Crystallogr.*, **A47**, 392–400.
Ewart,K.V., Rubinsky,B. and Fletcher,G.L. (1992) Structural and functional similarity between fish antifreeze proteins and calcium-dependant lectins. *Biochem. Biophys. Res. Comm.*, **185**, 335–340.
Graves, B.-J. *et al.* (1994) Insight into E-selectin/ligand interaction from the crystal structure and mutagenesis of the lec/EGF domains. *Nature*, **367**, 532–538.
Gross,J., Carlson,R.I., Brauer,A.W., Margolies,M.N., Warshaw,A.L. and Wands,J.R. (1985) Isolation, characterization, and distribution of an unusual pancreatic human secretory protein. *J. Clin. Invest.*, **76**, 2115–2126.
Iovanna,J., Frigerio,J.M., Dusetti,N., Ramare,F., Raibaud,P. and Dagorn,J.C. (1993) Lithostathine, an inhibitor of $CaCO_3$ crystal growth in pancreatic juice, induces bacterial aggregation. *Pancreas*, **8**, 597–601.
Itoh,T. *et al.* (1990) Isolation and characterization of human *reg* protein produced in *Saccharomyces cerevisiae*. *FEBS Lett.*, **272**, 85–88.
Jones,T.A., Zou,J.-Y., Cowan,S.W. and Kjeldgaard,M. (1991) Improved methods for building protein models in electron density maps and the location of errors in these models. *Acta Crystallogr.*, **D47**, 110–119.
Kraulis,P.J. (1991) MOLSCRIPT: a program to produce both detailed and schematic plots of protein. *J. Appl. Crystallogr.*, **24**, 946–950.
Leslie,A.G.W. (1987) Profile fitting. In Helliwell,J.H., Machin,P.A. and Papiz,M.Z. (eds), *Computational Aspects of Protein Crystal Data Analysis*. Proceedings of the Daresbury Study Weekend 23–24 January, 1987, pp 39–50.
Moore,E.W. and Vérine,H.J. (1987) Pancreatic calcification and stone formation: a thermodynamic model of calcium in pancreatic juice. *Am. J. Physiol.*, **252**, 707–718.
Ng,N.F.L. and Hew,C.L.(1992) Structure of an antifreeze polypeptide from the sea raven. *J. Biol. Chem.*, **267**, 16069–16075.
Nicholls,A., Sharp,K.A. and Honig,B. (1991) Protein folding and association: insights from the interfacial and thermodynamic properties of hydrocarbons. *Prot. Struct. Funct. Genet.*, 11, 281–296.
Ozturk,M., De La Monte,S., Gross,J. and Wands,J.R. (1989) Elevated levels of an exocrine pancreatic thread protein in Alzheimer disease brain. *Proc. Natl Acad. Sci.*, **86**, 419–423.
Patthy,L. (1988) Homology of human pancreatic stone protein with animal lectins. *Biochem J.*, **253**, 309–311.
Petersen,T.E. (1988) The amino-terminal domain of thrombomodulin and pancreatic stone protein are homologous with lectins. *FEBS Lett.*, **231**, 51–53.
Pignol,D., Bertrand,J.A., Bernard,J.-P., Verdier,J.-M., Dagorn,J.-C. and Fontecilla-Camps,J.C. (1995) Crystallization and preliminary crystallographic study of human lithostathine. *Prot. Struct. Funct. Genet.*, **23**, 604–606.
Ramachadran,G.N., Ramakrishnan,C. and Sasisekharan,V. (1963) Stereochemistry of polypeptide chain configurations. *J. Mol. Biol.*, **7**, 95–99.
Sheriff,S., Chang,C.Y. and Ezekowitz,R.A.B. (1994) Human mannose-binding protein carbohydrate recognition domain trimerizes through a triple α-helical coiled coil. *Natl Struct. Biol.*, **11**, 789–794.
Sicheri,F. and Yang,D.S.C. (1995) Ice-binding structure and mechanism of an antifreeze protein from winter flounder. *Nature*, **375**, 427–431.
Sönnichsen,F.D., Sykes,B.D., Chao,H. and Davies,P.L. (1993) The nonhelical structure of antifreeze protein type III. *Science*, **259**, 1154–1157.
Sönnichsen,F.D., Sykes,B.D. and Davies,P.L. (1995) Comparative modeling of the three-dimensional structure of type II antifreeze protein. *Protein Sci.*, **4**, 460–471.
Stewart,T.A. (1989) The human *reg* gene encodes pancreatic stone protein. *Biochem. J.*, **260**, 622–623.
Terazono,K., Yamamoto,H., Takasawa,S., Shiga,K., Yonemura,Y., Tochino,Y. and Okamoto,H. (1988) A novel gene activated in regenerating islets. *J. Biol. Chem.*, **263**, 2111–2114.
Watanabe,T., Yonekura,H., Terazono,K., Yamamoto,H. and Okamoto,H. (1990) Complete nucleotide sequence of human *reg* gene and its expression in normal and tumorial tissues. *J. Biol. Chem.* **265**, 7432–7439.
Weis,W.I. and Drickamer,K. (1994) Trimeric structure of a C-type mannose-binding protein. *Structure* **2**, 1227–1240.
Weis,W.I., Kahn,R., Fourme,R., Drickamer,K. and Hendrickson,W.A. (1991) Structure of the calcium-dependent lectin domain from a rat mannose-binding protein determined by MAD phasing. *Science*, **254**, 1608–1615.
Weis,W.I., Drickamer,K. and Hendrickson,W.A. (1992) Structure of C-type mannose-binding protein complexed with an oligosaccharide. *Nature*, **360**, 127–134.
Yang,D.S.C., Sax,M., Chakrabartty,A. and Hew,C.L. (1988) Crystal structure of an antifreeze polypeptide and its mechanistic implications. *Nature*, **333**, 232–237.
Zhang,K.Y.J. (1993) SQUASH-combining constraints for macromolecular phase refinement and extension. *Acta Crystallogr.*, **D49**, 213–222.

Received on December 14, 1995; revised on January 24, 1996